Research article

Unique clonal relationship between T-cell acute lymphoblastic leukemia and subsequent Langerhans cell histiocytosis with *TCR* rearrangement and *NOTCH1* mutation

Yuichi Yokokawa,[1,3] Tomohiko Taki,[1*] Masaharu Akiyama,[3,4*] Satoru Kobayashi,[2] Hisao Nagoshi,[2] Yoshiaki Chinen,[2] Akira Morimoto,[5] Hiroyuki Ida,[3] Masafumi Taniwaki[2]

[1]Department of Molecular Diagnostics and Therapeutics, and [2]Department of Molecular Hematology and Oncology, Kyoto Prefectural University of Medicine Graduate School of Medical Science, Kyoto, Japan

[3]Department of Pediatrics, and [4]Division of Molecular Genetics, Institute of DNA Medicine, The Jikei University School of Medicine, Tokyo, Japan

[5]Department of Pediatrics, Jichi Medical University School of Medicine, Shimotsuke, Tochigi, Japan

*Correspondence to: Tomohiko Taki, MD, PhD, Department of Molecular Diagnostics and Therapeutics, Kyoto Prefectural University of Medicine Graduate School of Medical Science, 465 Kajii-cho Kawaramachi-Hirokoji, Kamigyo-ku, Kyoto 602-8566, Japan.

Tel: +81-75-251-5659, Fax: +81-75-251-5659, E-mail: taki-t@umin.net

Masaharu Akiyama, MD, PhD, Department of Pediatrics, The Jikei University School of Medicine, 3-25-8 Nishi-shinbashi, Minato-ku, Tokyo 105-8461, Japan.

Tel: +81-3-3433-1111, Fax: +81-3-3435-8665, E-mail: makiyama@jikei.ac.jp

Running title: Clonality of LCH following T-ALL

Supported by: a Grant-in-Aid for Scientific Research (C) from the Ministry of Education, Culture, Sports, Science and Technology of Japan

Keywords: acute lymphoblastic leukemia; Langerhans cell histiocytosis; T-cell receptor γ; *NOTCH1* gene

ABSTRACT

Acute lymphoblastic leukemia (ALL) occasionally develops before or after the onset of Langerhans cell histiocytosis (LCH). The mechanism of LCH developing after ALL remains unclear; thus the clonality of LCH developing during maintenance chemotherapy for T-cell ALL (T-ALL) was investigated. The T-ALL and LCH cells tested had the same T-cell receptor (*TCR*) gamma rearrangement. Mutation analysis of the *NOTCH1* gene revealed 7213C>T (Q2405X) in exon 34 in T-ALL and LCH cells, but 5156T>C (I1719T) in exon 27 only in T-ALL. Polymerase chain reaction-restriction fragment length polymorphism analysis revealed three patterns of *NOTCH1* mutations in T-ALL cells. The results suggest that the T-ALL and LCH cells were derived from a common precursor with *TCR* rearrangement and a single *NOTCH1* mutation, rather than LCH cells developing from a minor clone of T-ALL with single *NOTCH1* mutation.

INTRODUCTION

Langerhans cell histiocytosis (LCH) is characterized by abnormal accumulation or proliferation of Langerhans cells and is a rare disease of unknown cause that occurs primarily in childhood (Howarth et al., 1999). Malignancies such as acute leukemia, malignant lymphoma, and solid tumors, rarely develop before or after the onset of LCH (Egeler et al., 1993, 1998). The Histiocyte Society reported 54 cases of LCH complicated with malignancies: 29 cases of acute leukemia, 4 of malignant lymphoma, and 21 of solid tumors (Egeler et al., 1998). LCH following T-cell acute lymphoblastic leukemia (T-ALL) is very rare, and the Berlin-Frankfurt-Munster study group reported that histiocytic disorders develop in 6 of 971 patients with T-ALL (Trebo et al., 2005). The mechanism of LCH developing after ALL remains unclear; suggested mechanisms include chemotherapy-induced immunological suppression, tumorigenesis of stem cells, secondary neoplasm, and genetic factors (Trebo et al., 2005). In this study, we analyzed a pediatric case of LCH that developed during maintenance chemotherapy for T-ALL.

MATERIALS AND METHODS

Clinical Description of the Patient

A 7-year-old Japanese boy was admitted to the Jikei University Hospital because of general fatigue and abdominal pain. The initial blood count showed hyperleukocytosis (235,300/μl; blastic cells, 94%) and thrombocytopenia of 5.1 x 10^4/μl. Bone marrow examination revealed hypercellularity (1,136 × 10^3/μl) with 90% lymphoblastic cells. Immunophenotypic analysis revealed high expression of T-cell markers: CD1 (53.1%), CD2 (97.9%), CD3 (79.1%), CD4 (1.4%), CD5 (97.3%), CD7 (98.3%), CD8 (2.2%), CD34 (20.9%) and HLA-DR (17.0%), and he was diagnosed as having T-ALL. Cytogenetic analysis of bone marrow demonstrated a normal karyotype (46,XY [20/20]). He was treated on the

HEX regimen as per the TCCSG ALL07-16-02 protocol. Twenty-two months after diagnosis of T-ALL, the patient, now 9-year-old, presented with flesh-colored papules, 3-5 mm in diameter, on the trunk and upper and lower extremities that resembled those of molluscum contagiosum (Supporting Information Fig. S1A) and gradually increased in both size and number. A skin biopsy revealed a dermal and epidermotropic infiltrate comprised of Langerhans cells (Supporting Information Fig. S1B and C) that expressed S100 (Supporting Information Fig. S1D) and CD1a (Supporting Information Fig. S1E). In addition, 24.9% of the infiltrating cells were positive for MIB-1. However, malignant cytological features such as hyperchromatic nuclei, prominent nucleoli, and atypical mitoses were not detected. Electron microscopy demonstrated the presence of Birbeck granules (Supporting Information Fig. S1F), which confirmed the diagnosis of LCH.

Eight weeks after the skin rash developed, the patient was readmitted because of 2 weeks of persistent dry cough and dyspnea. There were papules on the trunk and upper and lower extremities but no lymphadenopathy or organomegaly. There were no blast cells or hemophagocytosis in bone marrow specimens. A chest X-ray showed mild infiltrations in both lower lung fields (Supporting Information Fig. S2A), whereas computed tomography (CT) showed vascular enhancement and subtle interlobular septal thickening without ground-glass opacities or consolidation (Supporting Information Fig. S2B). A whole-body bone X-ray examination and bone scintigraphy revealed no LCH involvement. All tests for suspected pathogens were negative, including those for cytomegalovirus, Candida, Aspergillus, and P. jiroveci. The patient was treated with intravenous ampicillin/sulbactam, oral azithromycin and an inhaled corticosteroid. As the patient required continuous oxygen supplementation, treatment with intravenous methylprednisolone (3 doses of 1 mg/kg/day for 3 days) was started and was followed by treatment with intaravenous prednisolone (1 mg/kg/day). These treatments did not affect the respiratory symptoms. Induction

chemotherapy for LCH per the JLSG-02 protocol of the Japan LCH Study Group (cytosine arabinoside, vincristine, and predonisone) (Imashuku et al., 2009) was started 18 days after readmission; however, skin lesions increased in size and number, and respiratory symptoms worsened. CT scans of the chest showed progressive enhancement of vascular images and interlobular septal thickening 3 weeks after readmission (Supporting Information Fig. S2C), and widespread interstitial lesions with ground-glass opacities and interlobular septal thickening 4 weeks after readmission (Supporting Information Fig. S2D). Echocardiography showed high systolic pressure in the pulmonary artery (60 to 70 mmHg) and right ventricular hypertrophy, suggesting severe pulmonary hypertension. Mechanical ventilation with nitric oxide inhalation (15 to 20 ppm) was started since artery blood gas analysis showed acute respiratory distress syndrome: PaO2/FiO2 ratio of 156 and A-aDO2 of 425 mmHg on 90% oxygen. The patient's condition deteriorated rapidly and he died of respiratory failure 5 weeks after readmission. The patient's parents refused consent for autopsy.

The bone marrow cells at the onset of T-ALL and the skin biopsy specimens of LCH were analyzed after the informed consent was obtained in accordance with the Declaration of Helsinki, and the Institutional Review Board approved this study.

TCR Jγ Rearrangement Analyses by Southern Blot Analysis and Polymerase Chain Reaction

TCR Jγ rearrangement was analyzed using conventional Southern blotting and polymerase chain reaction (PCR) by commercial laboratory. DNA was extracted from frozen samples of bone marrow obtained at the onset of T-ALL and LCH by DNA Purification Kit (Promega, Madison, WI). Southern blot analysis for *TCRγ* rearrangements was performed with a probe for the J region of *TCRγ* and restriction enzymes of *Eco*RI, *Bam*HI and *Hind*III.

Mutational Analyses of *NOTCH1, FBXW7, BRAF*, and *MAP2K1* Genes

Mutations in *NOTCH1*, *FBXW7*, *BRAF*, and *MAP2K1* were analyzed in hot spots using PCR

followed by direct sequencing with some primers previously described (Park et al., 2009; Badalian-Very et al., 2010; Chakraborty et al., 2014). DNAs extracted from frozen bone marrow samples of T-ALL, and from paraffin-embedded skin biopsy specimens of LCH were used for analyses.

PCR-Restriction Fragment Length Polymorphism Analysis

Total RNA was extracted from frozen bone marrow samples of T-ALL with an ISOGEN LS Kit (Nippongene, Toyama, Japan), and cDNA was synthesized with Ready-To-Go You-Prime First-Strand Beads (GE Healthcare, Piscataway, NJ) in accordance with the manufacture's protocol. PCR-restriction fragment length polymorphism (RFLP) analysis was used to screen for *NOTCH1* mutations (exons 27 and 34). To detect the two *NOTCH1* mutations simultaneously, the following primers were used: HD-N1Fw2, PEST1Rv and HD-N2Fw2, TAD1Rv2 (Weng et al., 2004). Each reaction mixture (50 μl) contained 1μl of cDNA, 15 pmol of each primer, 10 μl of dNTPs mixture (2.0 mM each), 25 μl of 2×buffer and 1.0 U of KOD FX (TOYOBO, Osaka, Japan). Reaction conditions were as follows: initial denaturation at 94°C for 2 min followed by 30 cycles of denaturation at 98°C for 10 sec, annealing at 55°C for 30 sec, and extension at 68°C for 4 min. PCR products were run on a 1.0% agarose gel and visualized under UV illumination after SYBR-green staining.

PCR products were subcloned using TArget Clone -plus- (TOYOBO). Before subcloning, the 10× A-attachment mix was used to acquire overhanging dA at the 3'-ends since PCR products using KOD FX have blunt end. Subcloned products were amplified concurrently using the following primers: NOTCH Fw2, 5'-ACCGACGTGGCCGCATTCCT-3'; NOTCH 28R, 5'-AGCCCACGAAGAACAGAAGC-3' and NOTCH Direct F34, 5'-GTCCCAGATGATGAGCTACC-3'; TAD1RV2 (for exon34). One hundred nanograms of the PCR product was digested with 2 U of *Sau*3AI at 37°C and *Bsr*I at 63°C for 3 hr. Digested products were electrophoresed on a 3.0% agarose gel. A single band of exon 27 and double

fragment of exon 34 means that two mutations exist on the same allele.

RESULTS

Detection of the Same Clonal *TCR* Rearrangements, but Different *NOTCH1* Mutations in T-ALL and LCH

Southern blotting and genomic PCR analysis showed the same clonal *TCRγ* rearrangements in T-ALL and LCH cells (Fig. 1A and B). In addition, *NOTCH1* mutations in the PEST and extracellular heterodimerization (HD) domains: 7213C>T (Q2405X) was observed in the PEST domain (exon 34) in T-ALL and LCH, and 5156T>C (I1719T) in the HD domain (exon 27) in T-ALL (Fig. 1C). No mutations were detected in *FBXW7* (T-ALL), *BRAF* V600E (LCH), and exons 2 and 3 in *MAP2K1* (LCH).

Three Patterns of Aligned Relationship of Two *NOTCH1* Mutations

To determine whether the two mutations were aligned in *cis* or not, PCR-RFLP analysis was performed. Three patterns of *NOTCH1* mutations were identified: two mutations on the same allele (52%, 26/50 clones), a single mutation in exon 27 (16%, 8/50) and a single mutation in exon 34 (12%, 6/50) (Fig. 2A-C). The remaining 10 clones (20%) had no *NOTCH1* mutation. Additional analysis was performed in DND41, a T-ALL cell line, that has two *NOTCH1* mutations in the HD domain, 4781T>C (L1594P) and 4829A>T (D1610V). Sequencing of subcloned PCR products revealed two patterns of two *NOTCH1* mutations: two mutations on the same allele in 70 clones (70%), and a single 4781T>C mutation in one clone (1%) (Fig. 2D). The remaining 29 clones (29%) had no *NOTCH1* mutation.

DISCUSSION

The present study assessed the potential clonal relationship of T-ALL and LCH cells. The same clonal *TCRγ* rearrangements in T-ALL and LCH cells suggested the same clonal origin.

The pathogenetic relationship of LCH and ALL has rarely been reported. A case of LCH following T-ALL with identical clonal rearrangement of the *TCRγ* gene (Feldman et al., 2005) and other cases of LCH following non-Hodgkin's lymphoma with the same immunoglobulin heavy chain (*IGH*) gene rearrangement were reported previously (Magni et al., 2002; West et al., 2013). In addition, the case of a patient who developed LCH following T-ALL and in whom the same *TCR* rearrangement and *NOTCH1* mutations were observed was reported (Rodig et al., 2008). In these cases, identical gene alterations were detected in both T-ALL and LCH; however, in the present case, one of two *NOTCH1* mutations in T-ALL were absent in LCH. Although compound mutations in *NOTCH1* are typically aligned in *cis* in one of two alleles (Weng, et al., 2004; Aifantis et al., 2008), we initially supposed that double *NOTCH1* mutations in T-ALL cells might be present on different alleles and that one of these alleles might be lost during the differentiation from T-ALL into LCH. However, PCR-RFLP analysis in T-ALL cells detected three patterns of two *NOTCH1* mutations including two mutations on the same allele. These different patterns of *NOTCH1* mutations suggested the presence of homologous recombination, deletion or other events in T-ALL cells, and additional analysis in DND41 cell line also detected a clone with single *NOTCH1* mutation in addition to clones with two *NOTCH1* mutations. These findings usually suggest that the minor clone with the single *NOTCH1* mutation in exon 27 might be associated with LCH cells bearing the same mutation, and several papers recently reported the significance of minor subpopulations of leukemic cells at initial diagnosis in the development of relapse (van Delft et al., 2011; Bachas et al., 2012). The clonal relationship in our case of T-ALL with subsequent LCH is similar to that of these reported cases of de novo and relapsed leukemia; however, the relationship to disease phenotype in our case is quite different, suggesting that the LCH cells were not directly derived from a T-ALL cell.

The classical model of hematopoiesis holds that only early hematopoietic cells can

differentiate into both lymphocytes and phagocytes; however, recent analyses revealed that the progenitor cells at the branch point of the T-cell and B-cell lineages retain macrophage differentiation potential (Anjuere et al., 2000; Wada et al., 2008). The so-called transdifferentiation of B-lineage leukemia/lymphoma into histiocytic/dendritic malignancies with *IGH* rearrangements has also been reported (Magni et al., 2002; Feldman et al., 2008; Ratei et al., 2010; West et al., 2013). In addition, Chen *et al.* detected clonal rearrangements of *TCRγ,* immunoglobulin heavy chain or light chain in 30% (14 of 46) of patients with LCH who had not had leukemia/lymphoma either concurrently or in the past (Chen et al., 2010). Rearrangements of *TCRγ* and *IGH* detected in LCH cells suggest the same clonal origin of LCH and lymphoid neoplasms. In the light of these findings, our results suggested that the LCH cells of our patient were derived from a common precursor of T-ALL and LCH bearing *TCR* rearrangement and a single *NOTCH1* mutation (Fig. 3A), rather than developing from a minor clone of T-ALL with single *NOTCH1* mutation (Fig. 3B).

Recently, Castro et al. reported clinicopathological features of histiocytic lesions following ALL (Castro et al., 2010): the typical histiocytic lesions have a MIB-1 (Ki-67) less than 10%, the atypical histiocytic lesions have cytologic low-grade but have inappropriately higher nuclear pleomorphism, mitoses, and MIB-1 higher than 10%, and the Langerhans cell sarcoma (LCS) is cytologically high grade and the diagnosis of LCS was predicated on the malignant features by virtue of blastic appearance with a MIB-1 of 30-80% and phenotype such as CD14/CD68/CD163. In our patient, 24.9% of the infiltrating cells were positive for MIB-1, but malignant cytological features such as hyperchromatic nuclei, prominent nucleoli, and atypical mitoses were not detected. Thus, the LCH lesion of the skin in our patient was not diagnosable as a sarcoma.

The LCH of this patient was completely different from the common natural history of LCH. Our patient had multiple skin lesions of LCH with respiratory symptoms. Respiratory

symptoms gradually worsened, and the patient died of respiratory failure due to severe pulmonary hypertension. Pulmonary LCH is seen more than 30% of multisystem LCH, and that half of the patients have respiratory symptoms such as tachypnea, dyspnea, or wheeze (Odame et al., 2006). Pulmonary hypertension has been reported to complicate the course of nearly all patients with advanced pulmonary LCH (Rossi et al., 2014). However, it was difficult to diagnose pulmonary symptoms, because sequential chest CT showed no radiologic features of pulmonary LCH such as nodules and cysts in the lung parenchyma (Rao et al., 2010). The cause and mechanism of pulmonary hypertension remain unclear, because autopsy was not performed.

To our knowledge, only 14 cases of LCH that developed after ALL have been reported (Egeler et al., 1993; Chiles et al., 2001; Raj et al., 2001; Feldman et al., 2005; Trebo et al., 2005; Rodig et al., 2008; Mitsuki et al., 2010) (Table 1). Clinical data from these patients showed T-ALL predominance, a median interval between diagnoses of 12 months (range: 6 to 60 months), and an extremely poor prognosis for multi-system LCH (six of seven patients alive with single-system LCH and two of eight patients alive with multi-system LCH). In our patient, LCH developed during maintenance chemotherapy for T-ALL and responded poorly to the JLSG-02 protocol, which included prednisolone, vincristine and cytosine arabinoside (Imashuku et al. 2009), suggesting that it had already been resistant to these chemotherapeutic agents. One case with LCH following T-ALL having *NOTCH1* mutations has been reported, and its prognosis was also very poor (Rodig et al., 2008). In addition, one paper reported that *NOTCH1* is activated in lesional LCH, and suggested that the NOTCH ligand Jagged 2 (*JAG2)*-mediated NOTCH activation confers phenotypic and functional aspects of LCH to dendritic cells (Hutter et al., 2012). These findings suggest that the *NOTCH1* signaling play some roles in pathogenesis of LCH, and if so, *NOTCH1* inhibitors might have therapeutic benefit in LCH (Noguera-Troise et al., 2006; Hutter et al., 2012). Assessing clonality and

mutations in T-ALL and LCH may provide important clues to pathogenesis and treatment strategy in LCH following hematologic malignancy.

ACKNOWLEDGMENTS

The authors thank Professor Hiroshi Hano (Department of Pathology, The Jikei University School of Medicine), Dr. Nao Takagi (Department of Dermatology, The Jikei University School of Medicine), and Dr. Satoshi Matsushima (Department of Radiology, The Jikei University School of Medicine) for helpful suggestions and critical reading of the manuscript.

References

Aifantis I, Raetz E, Buonamici S. 2008. Molecular pathogenesis of T-cell leukaemia and lymphoma. Nat Rev Immunol 8: 380-390.

Anjuere F, del Hoyo GM, Martín P, Ardavín C. 2000. Langerhans cells develop from a lymphoid-committed precursor. Blood 96: 1633-1637.

Bachas C, Schuurhuis GJ, Assaraf YG, Kwidama ZJ, Kelder A, Wouters F, Snel AN, Kaspers GJ, Cloos J. 2012. The role of minor subpopulations within the leukemic blast compartment of AML patients at initial diagnosis in the development of relapse. Leukemia 26: 1313-1320.

Badalian-Very G, Vergilio JA, Degar BA, MacConaill LE, Brandner B, Calicchio ML, Kuo FC, Ligon AH, Stevenson KE, Kehoe SM, Garraway LA, Hahn WC, Meyerson M, Fleming MD, Rollins BJ. 2010. Recurrent BRAF mutations in Langerhans cell histiocytosis. Blood. 116: 1919-1923.

Castro ECC, Blazquez C, Boyd J, Correa H, De Chadarevian JP, Felgar RE, Graf N, Levy N, Lowe EJ, Manning Jr JT, Proytcheva MA, Senger C, Shayan K, Sterba J, Werner A, Surti U, Jaffe R. 2010. Clinicopathologic features of histiocytic lesions following ALL, with a review of the literature. Pediatr Dev Pathol 13: 225-237.

Chakraborty R, Hampton OA, Shen X, Simko SJ, Shih A, Abhyankar H, Lim KP, Covington KR, Trevino L, Dewal N, Muzny DM, Doddapaneni H, Hu J, Wang L, Lupo PJ, Hicks MJ, Bonilla DL, Dwyer KC, Berres ML, Poulikakos PI, Merad M, McClain KL, Wheeler DA, Allen CE, Parsons DW. 2014. Mutually exclusive recurrent somatic mutations in MAP2K1 and BRAF support a central role for ERK activation in LCH pathogenesis. Blood 124: 3007-3015.

Chen W, Wang J, Wang E, Lu Y, Lau SK, Weiss LM, Huang Q. 2010. Detection of clonal lymphoid receptor gene rearrangements in Langerhans cell histiocytosis. Am J Surg Pathol

34: 1049-1057.

Chiles LR, Christian MM, McCoy DK, Hawkins HK, Yen AH, Raimer SS. 2001. Langerhans cell histiocytosis in a child while in remission for acute lymphocytic leukemia. J Am Acad Dermatol 45: S233-234.

Egeler RM, Neglia JP, Puccetti DM, Brennan CA, Nesbit ME. 1993. Association of Langerhans cell histiocytosis with malignant neoplasms. Cancer 71: 865-873.

Egeler RM, Neglia JP, Aricò M, Favara BE, Heitger A, Nesbit ME, Nicholson HS. 1998. The relation of Langerhans cell histiocytosis to acute leukemia, lymphomas, and other solid tumors. The LCH-Malignancy Study Group of the Histiocyte Society. Hematol Oncol Clin North Am 12: 369-378.

Feldman AL, Berthold F, Arceci RJ, Abramowsky C, Shehata BM, Mann KP, Lauer SJ, Pritchard J, Raffeld M, Jaffe ES. 2005. Clonal relationship between precursor T-lymphoblastic leukaemia/lymphoma and Langerhans-cell histiocytosis. Lancet Oncol 6: 435-437.

Feldman AL, Arber DA, Pittaluga S, Martinez A, Burke JS, Raffeld M, Camos M, Warnke R, Jaffe ES. 2008. Clonality related follicular lymphomas and histiocytic/dendritic cell sarcomas: evidence for transdifferentiation of the follicular lymphoma clone. Blood 111: 5433-5439.

Howarth DM, Gilchrist GS, Mullan BP, Wiseman GA, Edmonson JH, Schomberg PJ. 1999. Langerhans cell histiocytosis. Diagnosis, natural history, management and outcome. Cancer 85: 2278-2290.

Hutter C, Kauer M, Simonitsch-Klupp I, Jug G, Schwentner R, Leitner J, Bock P, Steinberger P, Bauer W, Carlesso N, Minkov M, Gadner H, Stingl G, Kovar H, Kriehuber E. 2012. Notch is active in Langerhans cell histiocytosis and confers pathognomonic features on dendritic cells. Blood 120: 5199-5208.

Imashuku S, Kinugawa N, Matsuzaki A, Kitoh T, Ohki K, Shioda Y, Tsunematsu Y, Imamura T, Morimoto A; Japan LCH Study Group. 2009. Langerhans cell histiocytosis with multifocal bone lesions: comparative clinical features between single and multi-systems. Int J Hematol 90: 506-512.

Magni M, Di Nicola M, Carlo-Stella C, Matteucci P, Lavazza C, Grisanti S, Bifulco C, Pilotti S, Papini D, Rosai J, Gianni AM. 2002. Identical rearrangement of immunoglobulin heavy chain gene in neoplastic Langerhans cells and B-lymphocytes: evidence for a common precursor. Leuk Res 26: 1131-1133.

Mitsuki N, Kajiwara M, Nagasawa M, Morio T, Mizutani S. 2010. A case of Langerhans cell histiocytosis following acute lymphoblastic leukemia. Jpn J Pediatr Hematol 24: 93-96.

Noguera-Troise I, Daly C, Papadopoulos NJ, Coetzee S, Boland P, Gale NW, Lin HC, Yancopoulos GD, Thurston G. 2006. Blockage of Dll4 inhibits tumour growth by promoting non-productive angiogenesis. Nature 444: 1032-1037.

Odame I, Li P, Lau L, Doda W, Noseworthy M, Babyn P, Weitzman S. 2006. Pulmonary Langerhans cell histiocytosis: a variable disease in childhood. Pediatr Blood Cancer 47: 889-893.

Park MJ, Taki T, Oda M, Watanabe T, Yumura-Yagi K, Kobayashi R, Suzuki N, Hara J, Horibe K, Hayashi Y. 2009. *FBXW7* and *NOTCH1* mutations in childhood T cell acute lymphoblastic leukemia and T cell non-Hodgkin lymphoma. Br J Haematol 145: 198-206.

Raj A, Bendon R, Moriarty T, Suarez C, Bertolone S. 2001. Langerhans cell histiocytosis following childhood acute lymphoblastic leukemia. Am J Hematol 68: 284-286.

Rao RN, Moran CA, Suster S. Histiocytic disorders of the lung. 2010. Adv Anat Pathol 17: 12-22.

Ratei R, Hummel M, Anagnostopoulos I, Jähne D, Arnold R, Dörken B, Mathas S, Benter T, Dudeck O, Ludwig WD, Stein H. 2010. Common clonal origin of an acute

B-lymphoblastic leukemia and a Langerhans' cell sarcoma: evidence for hematopoietic plasticity. Hematologica 95: 1461-1466

Rodig SJ, Payne EG, Degar BA, Rollins B, Feldman AL, Jaffe ES, Androkites A, Silverman LB, Longtine JA, Kutok JL, Fleming MD, Aster JC. 2008. Aggressive Langerhans cell histiocytosis following T-ALL: clonally related neoplasms with persistent expression of constitutively active *NOTCH1*. Am J Hematol 83: 116-121.

Rossi A, Zompatori M, Tchouanhou PT, Amadori M, Palazzini M, Conficoni E, Galie N, Poletti V, Gavelli G. 2014. Rare causes of pulmonary hypertension: spectrum of radiological findings and review of the literature. Radiol Med 119: 41-53.

Trebo MM, Attarbaschi A, Mann G, Minkov M, Kornmuller R, Gadner H. 2005. Histiocytosis following T-acute lymphoblastic leukemia: a BFM study. Leuk Lymphoma 46: 1735-1741.

van Delft FW, Horsley S, Colman S, Anderson K, Bateman C, Kempski H, Zuna J, Eckert C, Saha V, Kearney L, Ford A, Greaves M. 2011. Clonal origins of relapse in ETV6-RUNX1 acute lymphoblastic leukemia. Blood 117: 6247-6254.

Wada H, Masuda K, Satoh R, Kakugawa K, Ikawa T, Katsura Y, Kawamoto H. 2008. Adult T-cell progenitors retain myeloid potential. Nature 452: 768-773.

Weng AP, Ferrando AA, Lee W, Morris JP 4th, Silverman LB, Sanchez-Irizarry C, Blacklow SC, Look AT, Aster JC. 2004. Activating mutations of *NOTCH1* in human T Cell acute lymphoblastic leukemia. Science 306: 269-271.

West DS, Dogan A, Quint PS, Tricker-Klar ML, Porcher JC, Ketterling RP, Law ME, McPhail ED, Viswanatha DS, Kurtin PJ, Dao LN, Ritzer RD, Nowakowski GS, Feldman AL. 2013. Clonally related follicular lymphomas and Langerhans cell neoplasms: expanding the spectrum of transdifferentiation. Am J Surg Pathol 37: 978-986.

FIGURE LEGENDS

Fig. 1. *TCR Jγ*rearrangements and *NOTCH1* mutations in T-ALL and LCH. (A) Southern blot analysis with a probe for the J region of *TCRγ*. Restriction enzymes are *Eco*RI in lane 1, *Bam*HI in lane 2, and *Hind*III in lane 3. Arrows show rearranged bands. (B) PCR analysis detected a common *TCR Jγ*rearrangement pattern in T-ALL and LCH. (C) *NOTCH1* mutations in T-ALL and LCH were detected by direct sequencing. The *NOTCH1* mutation 7213C>T (Q2405X) in exon 34 was detected in both T-ALL and LCH cells, while 5156T>C (I1719T) in exon 27 was found only in T-ALL. Black arrows and white arrows indicate mutated and wild-type nucleotides, respectively. CR, complete remission.

Fig. 2. Detection of the allelic pattern of two *NOTCH1* mutations. (A) PCR analysis was performed to detect two *NOTCH1* mutations simultaneously in our T-ALL patient. N1, N2, TAD and PEST are primers HD-N1Fw2, HD-N2Fw2, PEST1Rv and TAD1Rv2, respectively. (B) Method for PCR-RFLP analysis in this study. Subcloned PCR products were reamplified using the primers NOTCH Fw2, NOTCH28R for exon 27, NOTCH DIRECT F34, and TAD1Rv2 for exon 34. *Sau*3AI can digest the wild-type *NOTCH1* sequence in exon 27, but not the sequence with the point mutation 5156T>C. *Bsr*I cannot digest the wild-type *NOTCH1* sequence in exon 34, but can digest the sequence with the point mutation 7213C>T. A single fragment (210 bp) of exon 27 and double fragment (185 bp, 61 bp) of exon 34 means that two mutations exist on the same allele. (C) Electrophoresed digested products show both mutations in exons 27 and 34 (lanes 1, 3, 5, 6, 11, and 12), a single mutation in exon 27 (lanes 4 and 9), a single mutation in exon 34 (lanes 8 and 10), and no mutations in exons 27 or 34 (lanes 2 and 7). (D) Alignment relationship of the two mutations in DND41. Direct sequencing of exon 26 of *NOTCH1* in the DND41 cell line shows that the mutations 4781T>C (L1594P) and 4829A>T (D1610V) exist on the same allele (a), that no mutations

are present on the same allele (b), and that only a single mutation 4781T>C (L1594P) is present (c). Black arrows and white arrows indicate mutated and wild-type nucleotides, respectively.

Fig. 3. Two hypothetical processes from ALL to LCH. (A) Differentiation into T-ALL and LCH from a common progenitor. *TCR* rearrangement (a) and first *NOTCH1* mutation (7213C>T, Q2405X) (b1) occurred in the common precursor of T-ALL and LCH. Additional *NOTCH1* mutation (5156T>C, I1719T) may have induced T-ALL from a common precursor cell with *TCR* rearrangement and *NOTCH1* mutation Q2405X (b2), and some other mutations might be necessary for a common precursor cell with *TCR* rearrangement and *NOTCH1* mutation Q2405X to differentiate into LCH (c). (B) Differentiation into LCH from the minor clone of T-ALL. Both *NOTCH1* mutations occurred in the precursor of T-ALL (b), and other mutations may have induced LCH from a minor clone with *TCR* rearrangement and *NOTCH1* mutation Q2405X. R, rearrangement; mut, mutation.

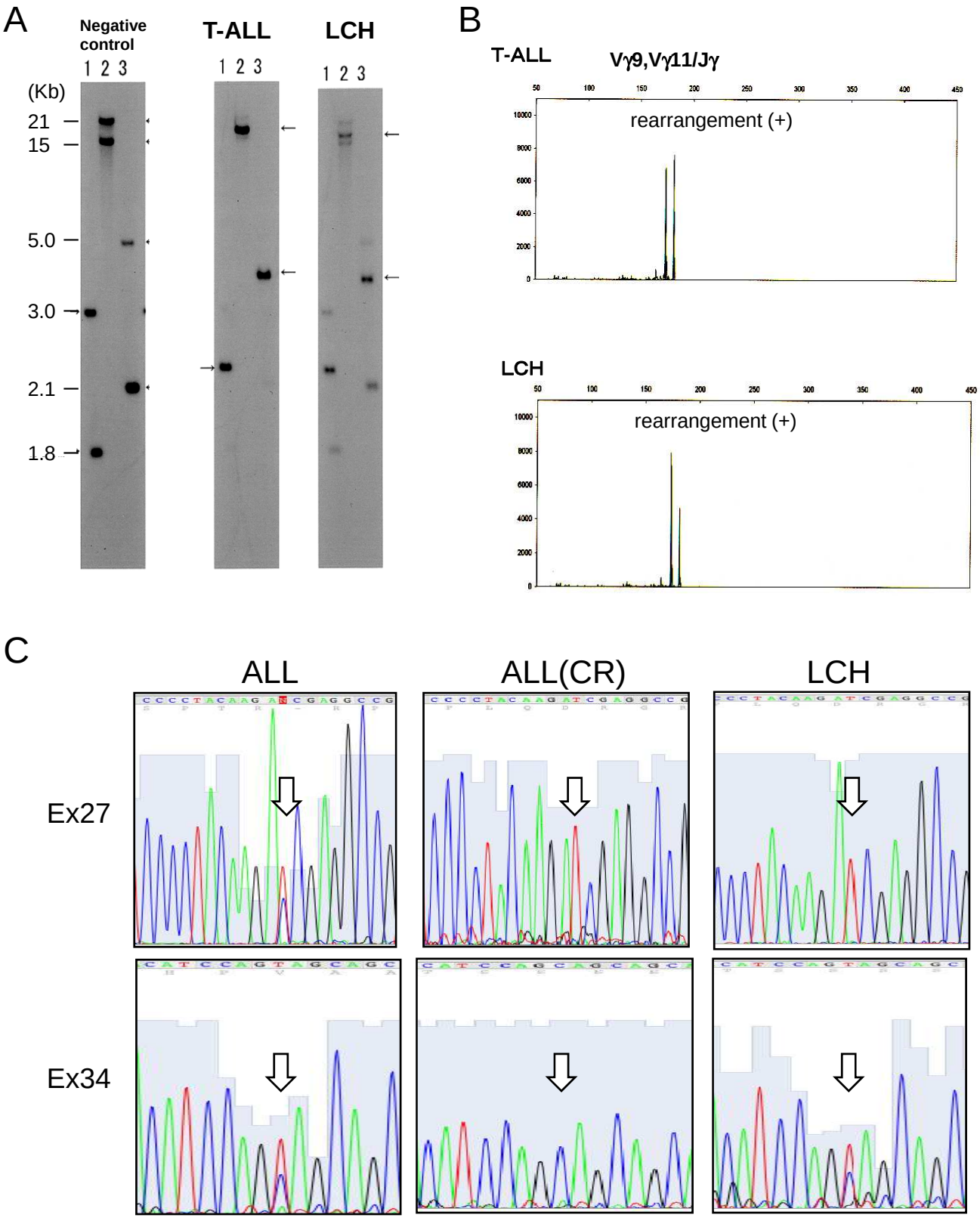
A
Negative control
T-ALL
LCH
1 2 3
(Kb)
21
15
5.0
3.0
2.1
1.8
B
T-ALL
Vγ9,Vγ11/Jγ
rearrangement (+)
LCH
rearrangement (+)
C
ALL
ALL(CR)
LCH
Ex27
Ex34

Figure 1

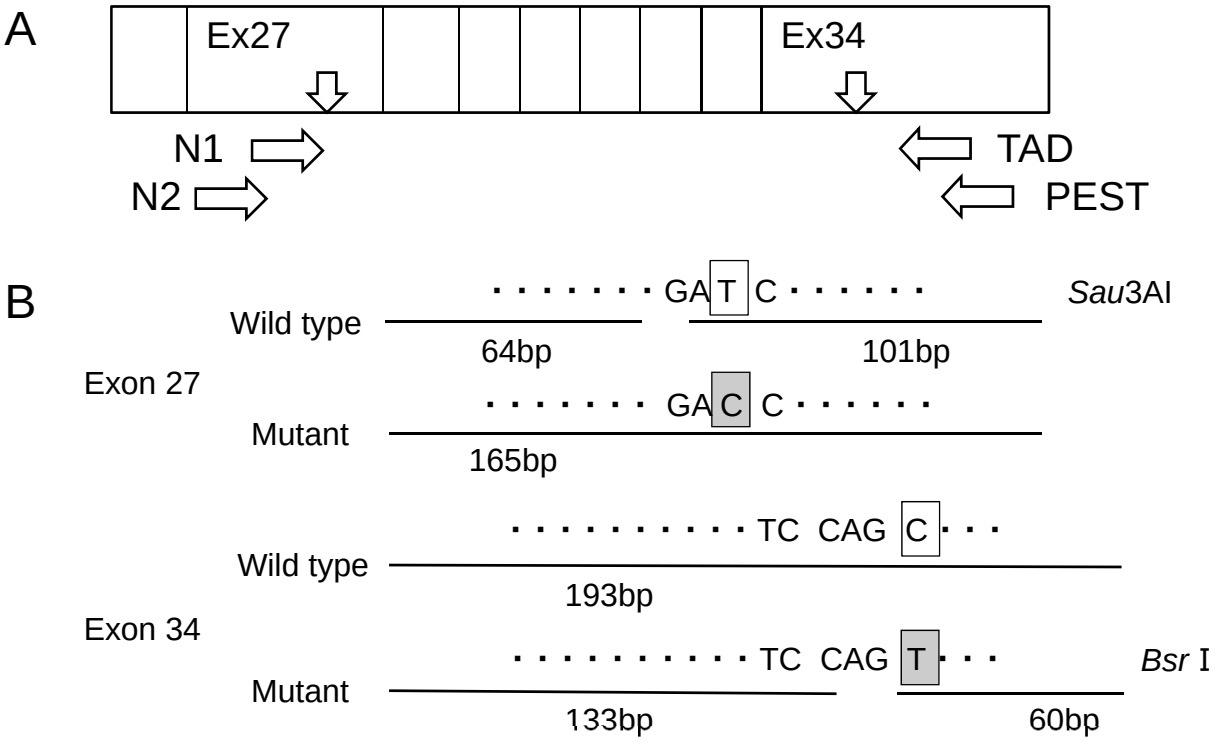
A
Ex27
Ex34
N1
N2
TAD
PEST
B
Wild type
GATC
Sau3AI
64bp
101bp
Exon 27
Mutant
GACC
165bp
TC CAG C
Wild type
193bp
Exon 34
TC CAG T
Bsr I
Mutant
133bp
60bp
C
M 1 2 3 4 5 6 7 8 9 10 11 12
(bp)
Exon 27
165
101
64
Exon 34
193
133
60
D
4781 T>C (+)
4829 A>T (+)
(a)
(b)
(c)

Figure 2

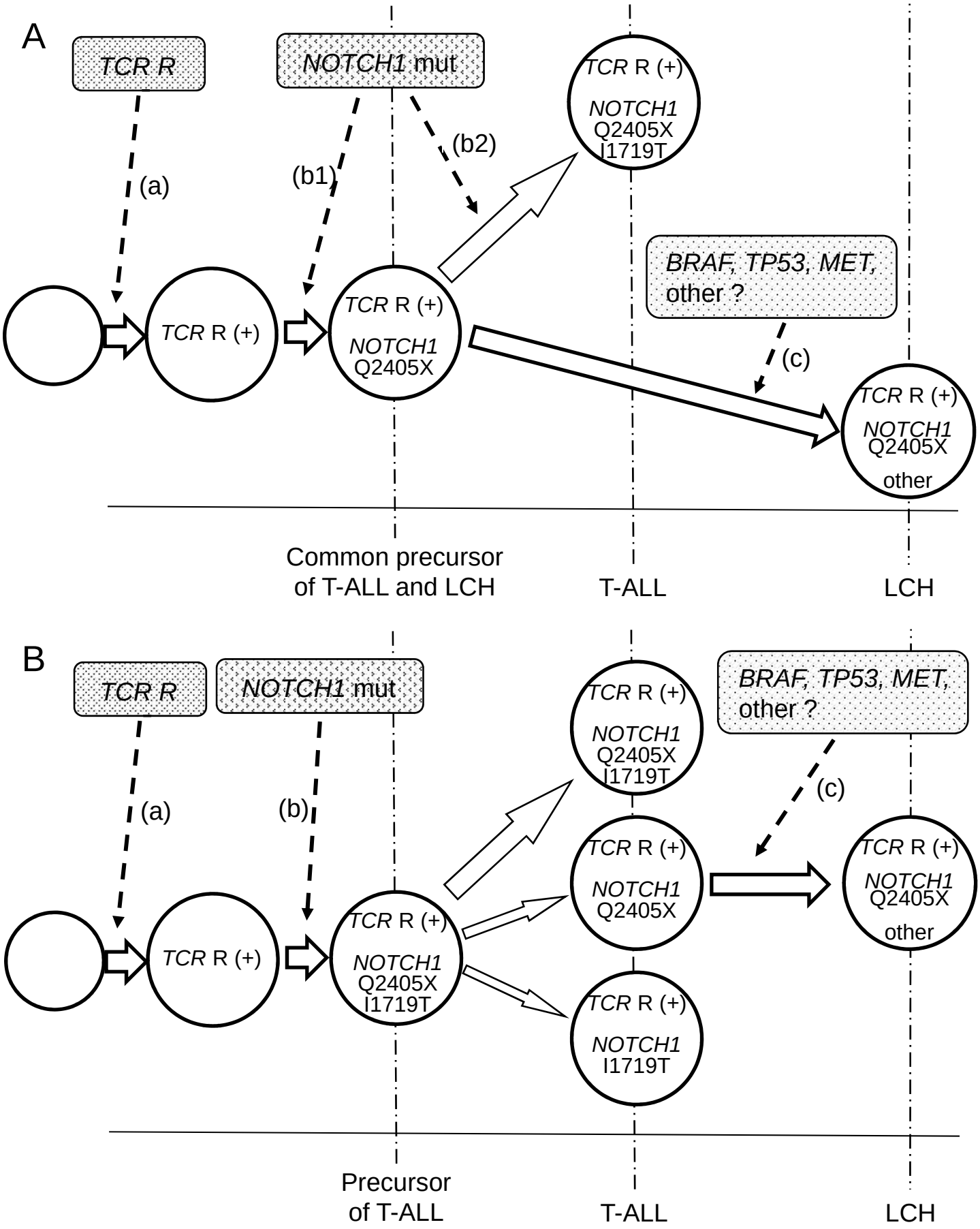
A
TCR R
NOTCH1 mut
(a)
(b1)
(b2)
TCR R (+)
NOTCH1
Q2405X
I1719T
TCR R (+)
NOTCH1
Q2405X
BRAF, TP53, MET,
other ?
(c)
TCR R (+)
NOTCH1
Q2405X
other
Common precursor
of T-ALL and LCH
T-ALL
LCH
B
TCR R
NOTCH1 mut
(a)
(b)
TCR R (+)
NOTCH1
Q2405X
I1719T
BRAF, TP53, MET,
other ?
(c)
TCR R (+)
NOTCH1
Q2405X
other
Precursor
of T-ALL
T-ALL
LCH

Figure 3

Table 1 : Summary of cases with LCH which developed after ALL.

Case	Age at diagnosis of ALL/SEX	Type	Karyotype of ALL	Time interval of LCH from ALL (months)	Site of LCH	Outcome of LCH (Cause of Death)	Reference No.
1	3/M	T	46,XY,del(9p)	12	Local (skin)	Alive	3
2	6/M	N/A	N/A	6	Generalized	Alive	3
3	4/F	N/A	N/A	12	Generalized	Death(LCH)	3
4	10/M	N/A	N/A	12	Generalized	Death(LCH)	3
5	3/M	N/A	N/A	12	Generalized	Death(LCH)	3
6	9/M	N/A	N/A	6	Generalized	Death(ALL)	3
7	13/M	N/A	N/A	6	Generalized	Alive	3
8	5/M	T	N/A	7	Generalized	Death(LCH)	21
9	5/M	T	N/A	31	Local (skin)	Alive	4
10	5/F	T	N/A	33	Local (skin)	Alive	4
11	5/M	T	N/A	28	Local (skin)	Alive	7
12	2/M	B	N/A	60	Local(bone)	Alive	22
13	8/F	B	*1	43	Local (skin)	Alive	20
14	3/F	T	N/A	18	Local (skin)	Death(Sepsis)	10
15	7/M	T	46,XY	22	Generalized (skin,lung?)	Death(LCH)	Our case

*[1] 51,XX,+4,+6,+8,i(17)(q10),+18,+21 [4/20]/52,XX,+X,+4,+6,+8,i(17)(q10),+18,+21[5/20]/46,XX [11/20]
M=male; F=female; N/A=not available

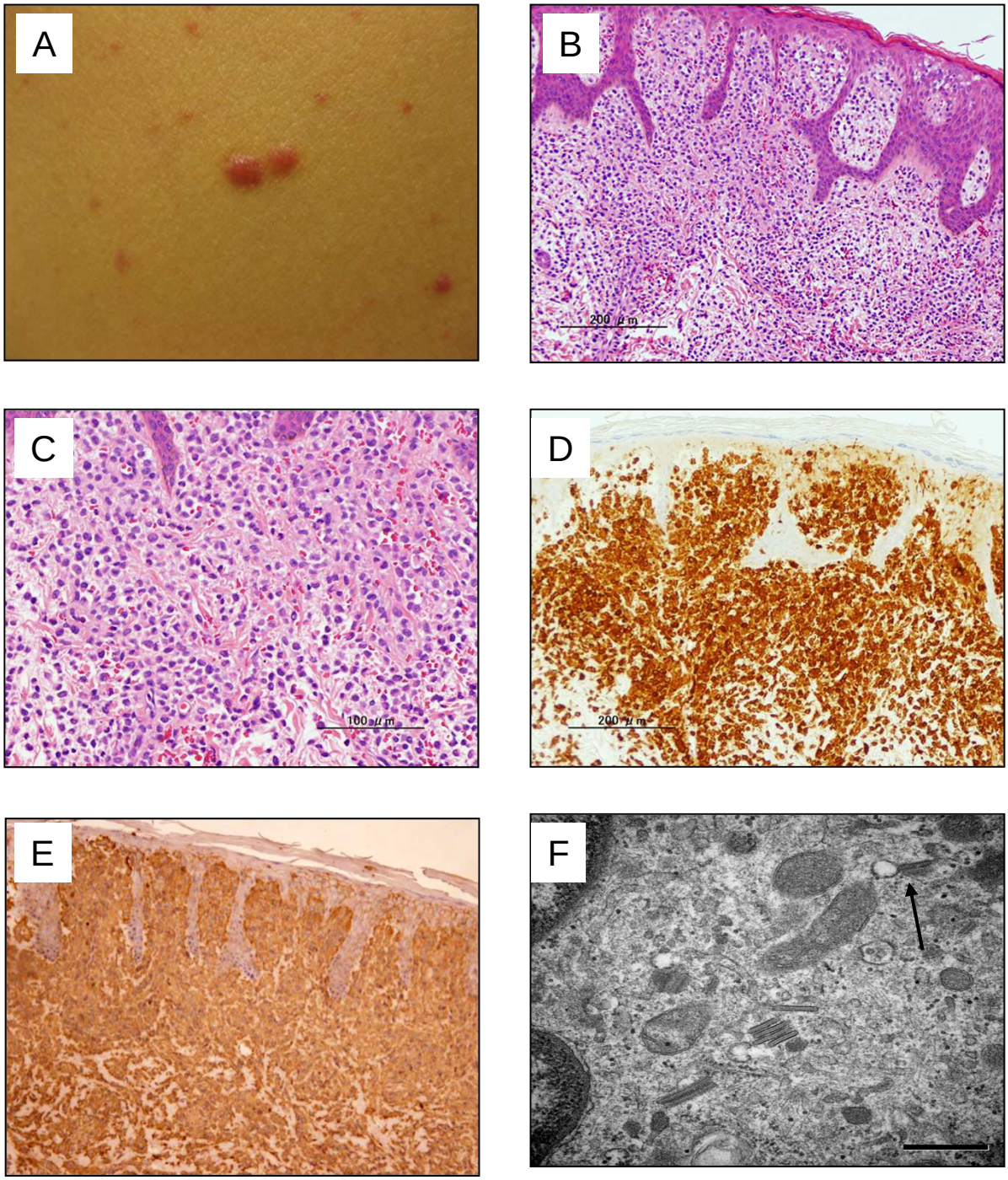

Supporting Information Figure S1. Morphologic characteristics and immunologic phenotype of the skin lesions. (A) Skin lesions seen at readmission, (B) hematoxylin and eosin stain (original magnification, x100), (C) hematoxylin and eosin stain (x400), (D) S100 (x100), (E) CD1a (x100), and (F) electron micrograph showing cytoplasmic Birbeck granules (arrows) (x50,000).

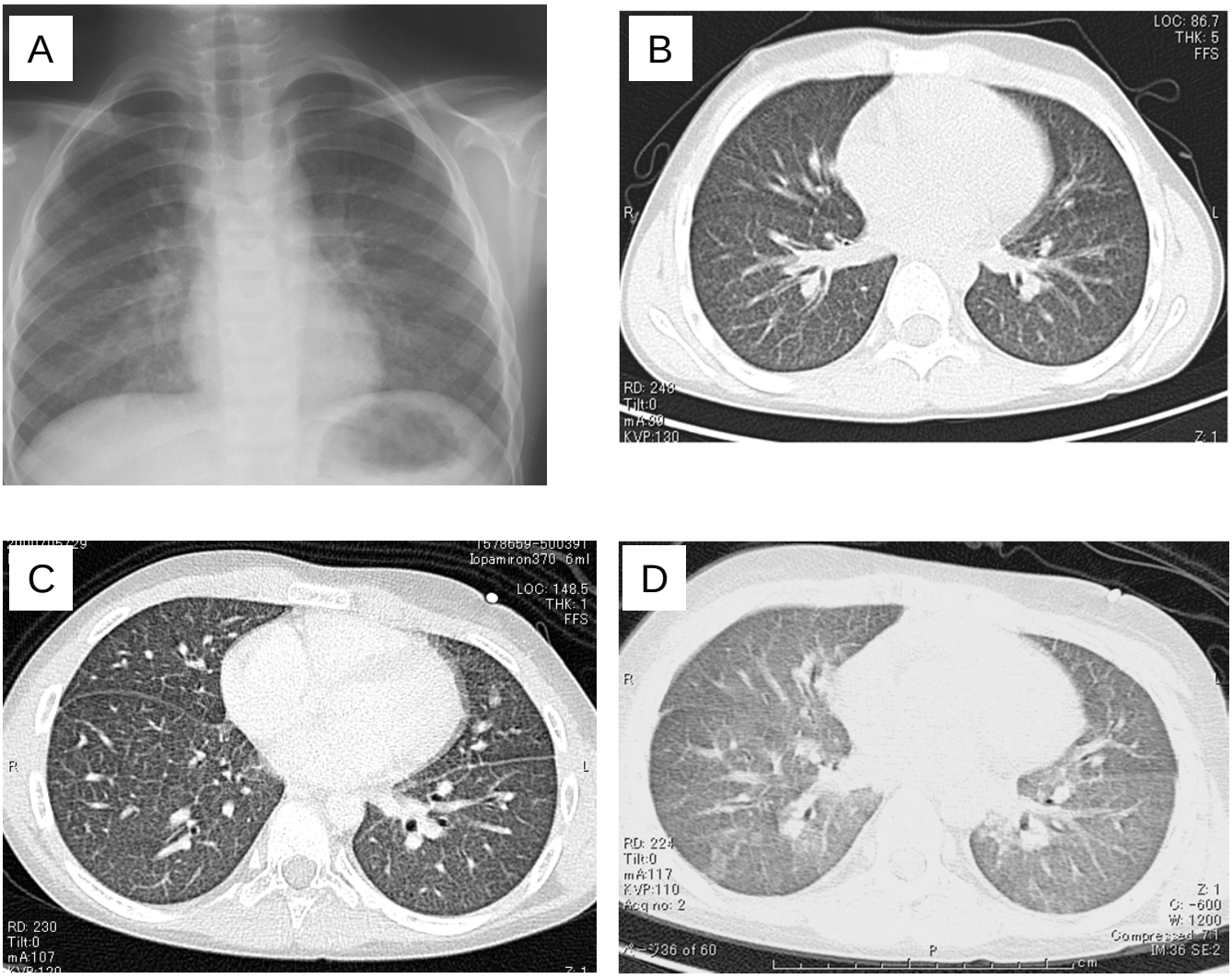

Supporting Information Figure S2. Radiologic examinations. Chest X-ray film (A) and CT on readmission (B), 3 weeks after readmission (C), and 4 weeks after readmission (D).